SANDIA REPORT
SAND2007-2287
Unlimited Release
Printed October 2007

Materials-Based Process Tolerances for Neutron Generator Encapsulation

D. B. Adolf, M. E. Stavig, and R. S. Berry

Prepared by
Sandia National Laboratories
Albuquerque, New Mexico 87185 and Livermore, California 94550

Sandia is a multiprogram laboratory operated by Sandia Corporation,
a Lockheed Martin Company, for the United States Department of Energy's
National Nuclear Security Administration under Contract DE-AC04-94AL85000.

Issued by Sandia National Laboratories, operated for the United States Department of Energy by Sandia Corporation.

Available to DOE and DOE contractors from
U.S. Department of Energy
Office of Scientific and Technical Information
P.O. Box 62
Oak Ridge, TN 37831

Telephone: (865) 576-8401
Facsimile: (865) 576-5728
E-Mail: reports@adonis.osti.gov
Online ordering: http://www.osti.gov/bridge

Available to the public from
U.S. Department of Commerce
National Technical Information Service
5285 Port Royal Rd.
Springfield, VA 22161

Telephone: (800) 553-6847
Facsimile: (703) 605-6900
E-Mail: orders@ntis.fedworld.gov
Online order: http://www.ntis.gov/help/ordermethods.asp?loc=7-4-0#online

SAND2007-2287
Unlimited Release
Printed October 2007

Materials-Based Process Tolerances for Neutron Generator Encapsulation

D. B. Adolf, M. E. Stavig, and R. S. Berry
Materials and Process Sciences Center
Sandia National Laboratories
Albuquerque, NM 87185

Abstract

Variations in the neutron generator encapsulation process can affect functionality. However, instead of following the historical path in which the effects of process variations are assessed directly through functional tests, this study examines how material properties key to generator functionality correlate with process variations. The results of this type of investigation will be applicable to all generators and can provide insight on the most profitable paths to process and material improvements. Surprisingly, the results at this point imply that the process is quite robust, and many of the current process tolerances are perhaps overly restrictive. The good news lies in the fact that our current process ensures reproducible material properties. The bad new lies in the fact that it would be difficult to solve functional problems by changes in the process.

1. Introduction

The current production process for neutron generator encapsulation was defined from years of experience, both fundamental and practical. One has difficulty arguing with its success based upon product reliability. However, the generator design itself has evolved over the years, and practical experience gained on previous generator versions may not directly carry over to the present design. In fact, we may have developed a "lore" surrounding the process that is somewhat imprecise. This imprecision, in turn, could lead to process tolerances that are either slightly off-target or overly restrictive. From a different perspective, when intermittent operational problems have been encountered in the generator, it is not uncommon for the cause to be assigned to the encapsulant or encapsulation process since historical "lore" suggests that small, ill-defined changes in the process or raw materials can affect large changes in generator performance. This study is aimed at re-investigating the encapsulation process tolerances from the perspective of material property requirements to assess the validity of our historical lore.

It is obvious both that the production process can affect encapsulant properties and that these properties can affect generator performance. We seem more accustomed historically to varying process parameters and directly measuring the effect on generator performance from functional tests. While this approach can assess effects of process changes, major drawbacks lie in the inability to apply directly the results from one generator design to another and the need to change only one parameter at a time. A more general approach would investigate both the effects of the process on material properties and the effects of material properties on generator performance. To define materials-based process tolerances, then, one first must identify those key material properties to which performance is sensitive. Following this, it is necessary to identify those process steps that affect these properties most severely. Finally, the sensitivity of the material properties to processing steps must be assessed. It is impractical to identify how all material properties are affected by processing and how performance depends on all these sensitivities; the parameter space is too massive. Rather, we must choose wisely and acknowledge that theoretical analysis can expand the effective range of the experimental data. The current

study begins this process, and most of the results are applicable as well to encapsulation processes other than neutron generators.

The first step toward defining materials-based process tolerances requires identification of those key encapsulant properties to which performance is sensitive. Successful generator performance will avoid mechanical failure of the encapsulant (cohesive or adhesive) during cure and subsequent thermal cycles, will ensure the proper high rate (shock) response of the encapsulant in ferroelectric generators, and will require that no dielectric breakdown occur during operation. Stresses both during and after cure obviously depend on the viscoelastic properties of the encapsulant and may depend on the extent of reaction. Adhesive and cohesive failure criteria determine when these stresses become critical and may also depend on the extent of reaction. Note that during cure, adhesion is required on some surfaces while de-bonding is desired on others, hence the use of mold releases. The high rate response of the encapsulant is most likely tied to quasi-static properties, but this relationship has not yet been fully determined. At present, shock response is examined by measuring only the longitudinal steady-state behavior (the Hugoniot). The unloading (or release) and non-longitudinal responses are also of interest but are not well understood.

Identifying material properties key to preventing dielectric breakdown during operation is likewise difficult since little insight exists into the underlying physics. Nevertheless, we do know that large voids trapped in the encapsulant during processing can act as initiation sites for dielectric breakdown. Since voids are more likely to be trapped in encapsulants with high viscosity, the sensitivity of viscosity to processing parameters is of interest not only for processing ease but for dielectric breakdown as well. Open cracks are possible breakdown sites linking the initiation of mechanical failure to electric failure. In electronic generators, the fabric spacers around the transformer must be fully saturated with epoxy to avoid breakdown in trapped voids, and permeability may vary with winding tension or fabric non-uniformity. Undoubtedly, other factors are important for breakdown, highlighting the need for further research into this area.

In general, then, the vision of materials-based process tolerances is clear. Examine the sensitivity of those properties deemed important for operation (mechanical failure, dielectric breakdown, high rate response,..) to process variations that could be expected. Process tolerances could reasonably be defined, for example, when the variations in a material property from intentional

changes in the process are statistically greater than those arising from multiple tests on material processed to the nominal specifications.

2. Sensitivities of material properties to selected materials analysis, storage, and preparation issues

2.1. Incoming materials analysis issues

All incoming materials are examined to ensure that they are indeed the correct chemical and that the quality meets our perceived requirements. One may wonder if the current tests limits are physically related to significant changes in material properties. As a start, examine those materials most important to encapsulation: "828" epoxy (diglycidyl ether of bisphenol A), "DEA" (diethanolamine) and "Z" curatives (4,4'-methylene-dianiline), "GMB" (glass microballoon) and "alox" (alumina) fillers, "CTBN" (carboxyl terminated butadiene acrylonitrile) rubber toughenener, mold releases, and transformer fabrics (for the electronic generator).

2.1.1 Epoxy and curatives

The reactivity of epoxy and curatives are ensured by wet chemical functionality tests, and additional tests such as viscosity and water or chlorine content ensure purity. The bounds on curative and epoxy functionalities are quite restrictive. For example, the amine nitrogen weight percent of the Z curative is controlled to ±1% of the theoretical value, and the weight per epoxy equivalent of the 828 is controlled to within ±2%. These tolerances are equivalent to the weighing requirements during processing and therefore, represent possible stoichiometric variations in the encapsulant.

The sensitivity of the cured encapsulant properties to variations in incoming functionality test results is mitigated by the universal properties of epoxies relative to their glass transition temperature. Restated, if one examines the thermophysical properties of epoxies at a fixed temperature difference below the glass transition, all systems appear quite similar. Table 1 lists the coefficients of thermal expansion (CTE), shear moduli, and bulk moduli of three common, unfilled, epoxy SNL encapsulants (Z, DEA, and "459") and five other unfilled epoxies (details given in the Appendix) all measured at roughly 90C below their

glass transition temperature, Tg. These linear viscoelastic properties vary little even with changes in system chemistry.

Table 1: Universality of the linear viscoelastic properties of various epoxies.

epoxy	CTE ($x10^{-4}$/C)	shear modulus (GPa)	bulk modulus (GPa)
828/Z	1.6 ± 0.1	1.2 ± 0.1	5.3 ± 0.2
828/DEA	1.7 ± 0.1	1.0 ± 0.1	5.4 ± 0.2
SNL 459	1.7 ± 0.1	1.3 ± 0.1	5.0 ± 0.2
815/3300	---	1.2 ± 0.1	---
862/T403	---	1.1 ± 0.1	---
826/3300	---	1.2 ± 0.1	---
828/aniline	1.6 ± 0.1	1.4 ± 0.1	5.4 ± 0.2
828/MEK peroxide	1.6 ± 0.1	1.3 ± 0.1	5.2 ± 0.2

The nonlinear and ultimate properties measured at 90C below Tg are also quite similar as shown in Table 2. The fracture toughness was measured in pre-cracked, three-point bend geometry, and the critical tangential adhesive strength was measured with the napkin ring test.

Table 2: Universality of the yield stress and failure metrics of various epoxies.

epoxy	compressive yield stress (MPa)	fracture toughness K_{IC}(psi-$in^{1/2}$)	critical tangential adhesive strength (MPa)
828/Z	---	610 ± 40	---
828/DEA	95 ± 5	630 ± 40	65 ± 10
SNL 459	90 ± 5	610 ± 40	55 ± 10
815/3300	---	620 ± 40	---
862/T403	---	700 ± 40	---
826/3300	---	690 ± 40	---
828/aniline	100 ± 5	---	---
828/MEK peroxide	95 ± 5	---	---

Note that it is imperative to measure properties at a constant temperature difference from Tg since many properties have sizeable temperature dependencies (Fig. 1), and the Tg's of these systems vary from 70 to 120C.

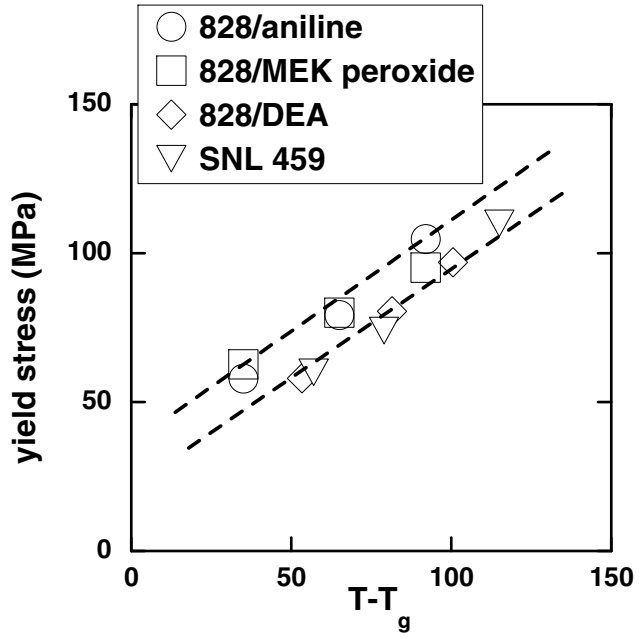

Fig. 1: The yield stress exhibits a significant dependence on temperature.

Since very slight changes in material properties are observed for curatives that include aliphatic amines, aromatic amines, cycloaliphatic amines, and even peroxides, one believes that minor variations in functionality (1-2%) allowed between incoming batches of the same reactant will result in imperceptible changes in the properties of the cured, unfilled encapsulants. Indeed, Fig. 2 shows that even the fracture toughness, which appeared to be the most sensitive property to changes in chemistry, is quite constant over modest variations in the extent of reaction that accompany stoichiometric variations. However, the Tg can change by ±10^{o}C over this range. Remember that the Tg's of the systems listed in Tables 1 and 2 varied by 50^{o}C as well.

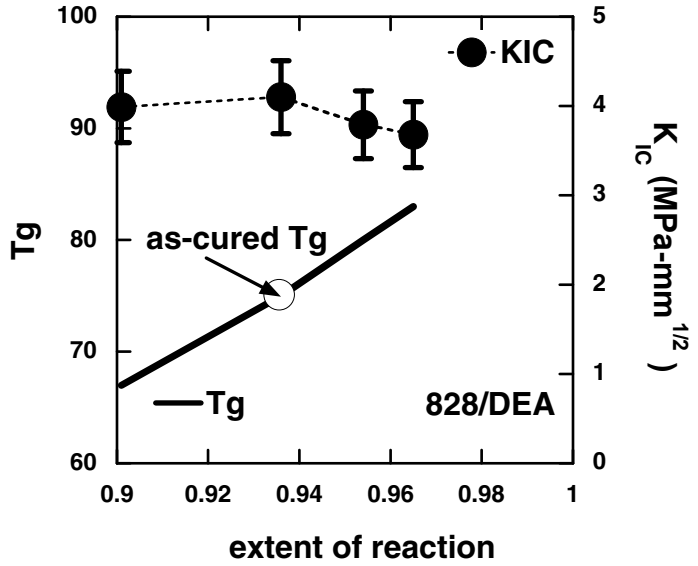

Fig. 2: Dependencies of Tg and fracture toughness (measured at 50C below the evolving Tg) on extent of reaction in the 828/DEA system.[1]

Two conclusions can be drawn from this discussion. First, the thermophysical properties of unfilled polymer appear to be quite universal when measured at a constant temperature difference below Tg. However, Tg itself can vary significantly from system to system and within a system as a function of extent of reaction or, equivalently, stoichiometry. Therefore, it appears that a reasonable screening test for assessing the sensitivity of cured epoxy properties to process or incoming material variations would be a simple measurement of Tg. Second, the bounds on the functionality of our incoming resins and curatives are easily sufficient to ensure reproducible cured properties, yet also easily satisfied from lot to lot.

2.1.2 Fillers

The glass microballoons fillers are tested for chemical composition (boron content and internal gas), size (sieving), volatile content, and density. Boron content is critical in certain instances but will not be discussed here. Size is important for dielectric breakdown concerns and will also not be discussed here. The key mechanical property is the density. Fig. 3 plots the vendor supplied hydrostatic crush strengths against particle density.

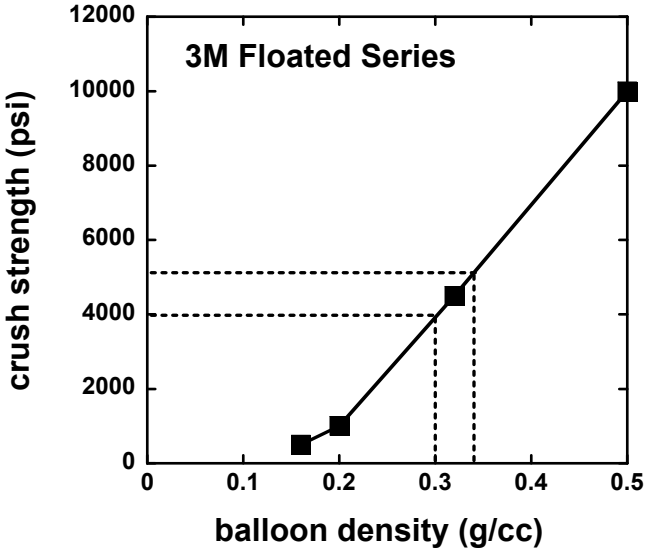

Fig. 3: Crush strengths of the 3M floated glass microballoons vs. particle density. The acceptable density range for the D32 series is highlighted.

Obviously, the higher density balloons have thicker walls and higher crush strengths. The incoming test limits on density allow at most a ±10% variation, which translates into roughly a ±10% variation in crush strength.

The crush strength has been shown to correlate with the mechanical failure stress in uniaxial compression for the DEA-cured, GMB-filled epoxy (Fig. 4).

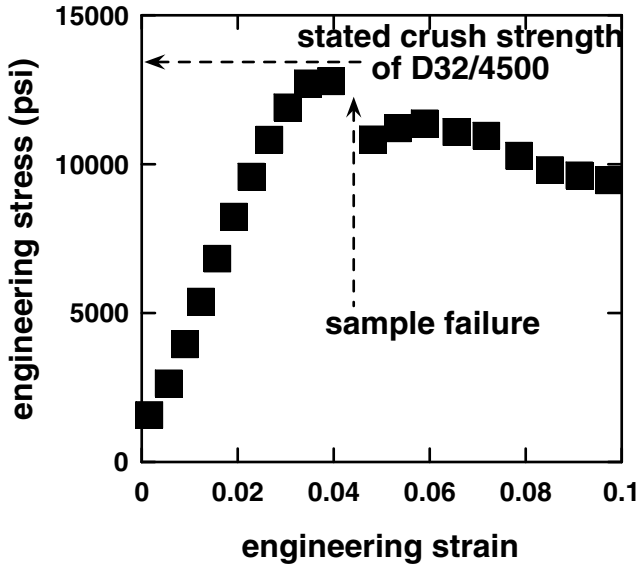

Fig. 4: GMB-filled 828/DEA fails at room temperature when the GMB crush.

In uniaxial compression, the pressure in the sample is three times the engineering stress. Since the nominal crush strength of our D32 GMB is 4500 psi, they should crush at a compressive stress of 13,500 psi as measured and plotted in Fig. 4. Remembering that the incoming test limits could allow for a ±10% variation in crush strength, the samples could fail at 12,000 psi instead of 13,500 psi. Since component designs, in general, should well exceed 10% margins, we feel comfortable in the test limits from a mechanical perspective.

The rubber-toughened epoxy precursor is produced at Kansas City (KC) from the Epon 828 epoxy resin and the carboxyl terminated butadiene acrylonitrile (CTBN) rubber. The rubber toughener is tested at KC, and the adduct is tested at SNL. We have historically noticed fluctuations in the acrylonitrile content of the rubber, which has caused separation problems. However, addition of the rubber toughener may be superfluous in GMB-loaded applications. It is well-documented that addition of CTBN to unfilled epoxies increases the fracture toughness. However, it appears that no such toughening occurs in GMB-loaded epoxies), and yet the addition of CTBN severely increases the processing viscosity (Table 3). Therefore, future use of CTBN is uncertain and no further investigations were pursued.

Table 3: Fracture toughnesses of CTBN-filled epoxies.[2]

system	K_{IC} (ksi-in$^{1/2}$)	initial viscosity at 70C (P)
828/DEA	0.63	2.9
828/CTBN/DEA	1.79	14.5
828/DEA/GMB	0.92	110
828/CTBN/DEA/GMB	0.85	350
828/Z	0.61	
828/CTBN/Z	1.80	
828/Z/GMB	1.10	
828/CTBN/Z/GMB	1.01	

The alumina filler has been closely scrutinized in recent investigations.[3] While large variations in the viscosity of various lots of Alcoa T64 alumina are observed (Fig. 5), these have not been correlated with the incoming test results on the alumina (chemical content, particle size, and particle density).

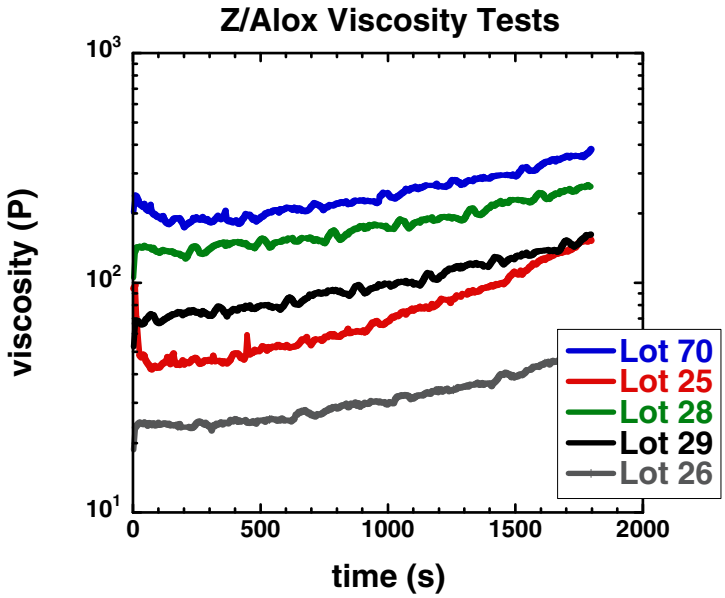

Fig. 5: Variations in the viscosity of 828/Z during cure filled with different lots of T64 alumina.

These observations led to an extensive and on-going study of the effects of varying alumina type on a wide range of encapsulant properties spanning quasi-

static viscoelastic response to high rate behavior to dielectric breakdown.[3] Considerable data gathered thus far indicate that even gross changes in alumina particle shape and size distribution have little effect on any properties (quasi-static, high-rate, or dielectric) except viscosity, which itself is a quite unexpected result. It might be reasonable, however, to incorporate a direct measurement of filled-epoxy viscosity into the incoming alox specifications, since excessive viscosities could result in incomplete degassing, trapped air, and possible dielectric breakdown sites. Therefore, a viscosity-based incoming material test is currently being developed.

2.1.3 Mold releases

RAM 225 was the mold release of choice for many years, only to be replaced recently by the Ultra II mold releases from Price-Driscoll. Use of RAM 225 was discontinued not only due to the methylene chloride carrier solvent (suspect carcinogen) but because systematic adhesion studies by T. Guess and M. Stavig demonstrated that Ultra II performed better.[4] Tests on incoming lots of RAM 225 included FTIR analyses and actual mold release adhesion strengths. The adhesion test requirements were not included in the new specification on Ultra II, since the procedure was laborious and no rejections of RAM based on this test could be remembered.

In the following discussion, six mold releases will be discussed: RAM 225, Ultra IIA (now used in place of the discontinued original Ultra II studied by Guess and Stavig), Ultra 3 and Ultra 4 (new versions of the Ultra line), and ME 515E and 515S (Zip-Chem Products). The carrier solvent in the original Ultra II, dichlorofluoroethane (a suspect ozone depleter), was replaced by isoparaffinic hydrocarbons in Ultra IIA. Since the hydrocarbons in Ultra IIA are flammable, Price-Driscoll released Ultra 3 containing n-propyl bromide and 1,1,1,2-tetrafluoroethane and Ultra 4 that replaced n-propyl bromide with dimethyl ether. The ME 515 products also both use a halogenated hydrocarbon/ether blend.

FTIR spectra of the six mold releases were obtained by Kathy Alam, 8333. The complete spectra are shown in Fig. 6, and the region of interest for siloxanes is enlarged in Fig. 7. All absorbances have been normalized by the Si-O-Si backbone contribution.

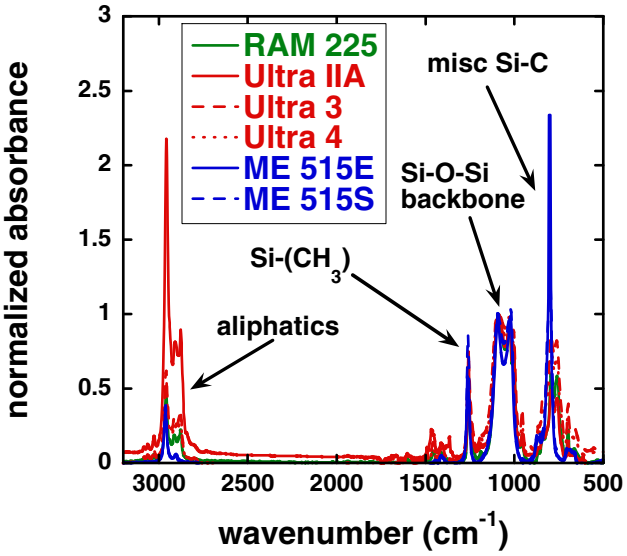

Fig. 6: FTIR absorbance spectra of the dried mold releases.

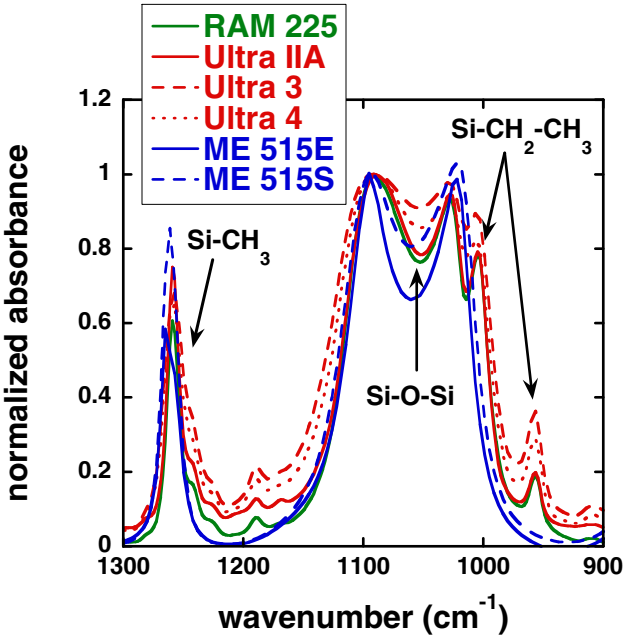

Fig. 7: The spectra of Fig. 6 are enlarged in the area of interest.

While some differences in the side groups and termination are noticeable, the compounds are predominantly polydimethylsiloxane.

The surface tensions of all six compounds were also measured with a du Nuoy Ring in Dept. 2453. It was thought that surface tension might be related to

the mechanism of mold release and be a sensitive yet easy test for performance (lower surface tension = better mold release). Each system was applied and then dried for at least 24 hours to ensure that the carrier solvents were evaporated. The results are shown in Table 4.

Table 4: Surface tensions of the dried mold releases

system	surface tension (mJ/m^2)
RAM 225	24.1
Ultra IIA	24.3
Ultra 3	24.1
Ultra 4	24.0
ME515E	21.3
ME515S	21.0

At this point, both FTIR and surface tension results show minor differences between products.

The above results would lead one to believe that the mold release performance of the six systems would be somewhat similar. A test geometry for assessing relative mold releasing characteristics uses an aluminum tube (1.5in I.D., 1.0in O.D., 3.2in tall) to which a thin (18mils) aluminum disk is attached with a screw-on cap (Fig. 8).

Fig. 8: Test geometry used for assessing the mold releasing performance of six different products.

The tube inner walls are sand-blasted, mold release is applied to the disk, and tube is filled with either 828/Z/alox or 828/CTBN/DEA/GMB encapsulant that is cured as described in Table 5.

Table 5: Encapsulants used in the mold release study.

system	weight ratios	cure profile
828/Z/Alox	100/20/300	2hr at RT, 10hr ramp to 93C, 10hr hold at 93C
828/CTBN/DEA/GMB	100/12/28	2hr at RT, 10hr ramp to 93C, 10hr hold at 93C

A strain gauge attached to the bottom of the thin disk measures displacements in the disk caused by cure stresses. When delamination occurs for each mold release investigated, the gauge reading will return to zero.

The critical strains at delamination are plotted in Fig. 9 for three of the six mold releases applied by wiping on the aluminum disk. Significant differences are seen in the mold releasing performances. Ultra 3 was not even tested since it never released from the preliminary aluminum test pans. Ultra 4 only released for the test pans when a heavy layer was applied; that is, the epoxy stuck to test pans when a light spray was applied.

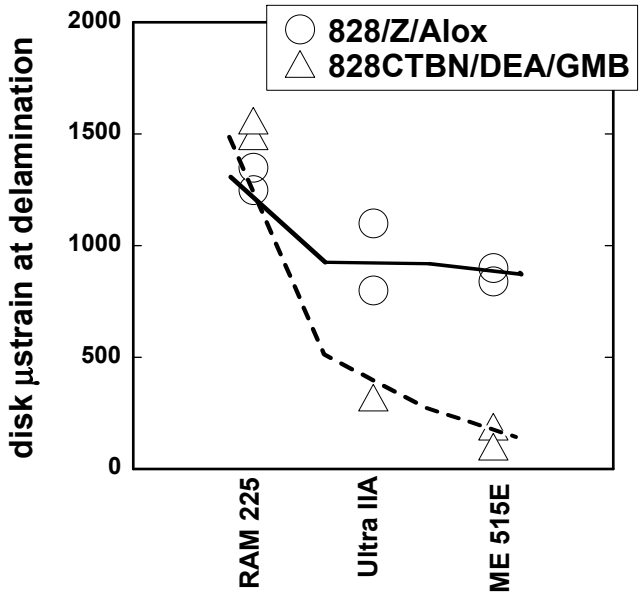

Fig. 9: Strains at delamination for various mold releases.

Examining just the Ultra IIA, 3, and 4 results, neither FTIR nor surface tension measurements showed measurable differences between the systems, yet there are gross differences in actual performance, which suggests that the carrier

solvent may be an important factor in mold release performance. Certainly the surface tension of the solvent and the solubility of the active ingredient in the solvent could be key factors in determining wetting. Kinetic effects during the evaporation process may also be important. Current investigations are focused on such issues. However, it seems prudent to extend the analyses of incoming mold release to re-institute FTIR of both the as-applied and dried material to ensure consistency in both the active ingredient and the carrier solvent.

2.1.4 Fabrics

The transformers in electronic generators have historically used a non-woven, polyester (Dacron, Webril M1483, Kendell Co.) fabric mat as the spacer between winding layers. Unfortunately, this particular product is no longer available, but several alternate materials have been identified. Historical incoming material tests include effective mat density, FTIR fiber analysis, and tensile strength. In the process of evaluating these new alternatives, we included in the screening process a new test to evaluate the rate of uptake of epoxy resin into the fabric. This new test was considered important since incomplete infiltration of the resin into the fabric could result in dielectric breakdown in a trapped void in the transformer.

The test is quite simple; strips of fabric are suspended by clamps in a heated oven (70C) such that the dangling ends are wetted by the resin (Fig. 10).

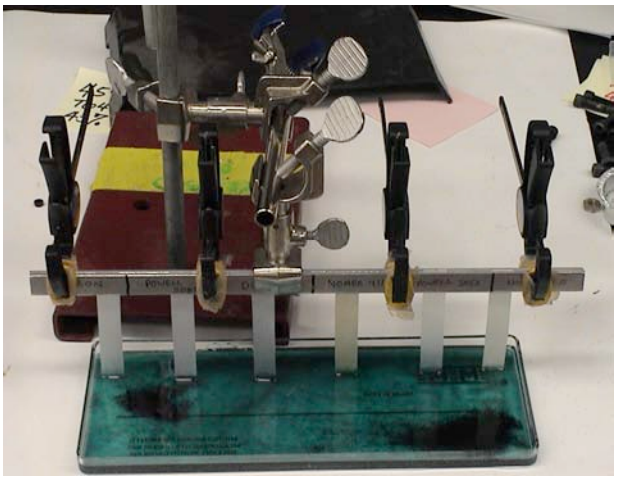

Fig. 10: Photo of the wicking test geometry for evaluating the relative infiltration rates of resin into transformer fabrics.

The resin will wick up the fabrics with time, and the front is clearly visible. Relative infiltration rates can be determined by plotting the front position versus time.

While several replacement fabrics were evaluated, two were nominally identical to the historical Dacron mat: Powell 5085 (Powell Corp.) and DSB-5 (Bedford Materials). All three products are non-woven polyester mats nominally 5 mils thick and with a density between 80 and 90 gms/yd^2. While variations in tensile strength could exist, one would think infiltration rates would be determined primarily by fabric type and density. Yet, the wicking of the resin varied significantly between the three products (Fig. 11).

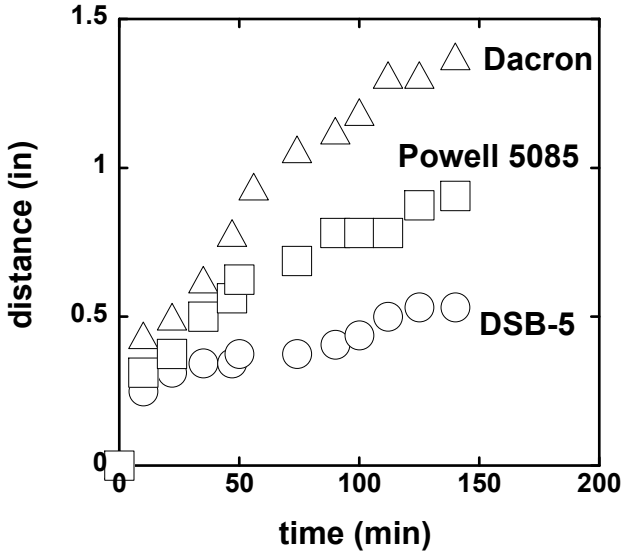

Fig. 11: Wicking of resin into nominally identical polyester fiber mats.

The reason for such variability is unclear. It could be due to unknown fiber surface treatments, for example.

Only one lot of material was available for testing for each of the fabrics. Thus, while the wicking rates were quite reproducible within each lot, the variability between lots of the same material could not be determined. If surface treatments varied from lot-to-lot, perhaps variations in infiltration would result and translate into possible performance variations. It is suggested that, when a replacement material is selected, wicking tests be pursued for a while to assess consistency of the product.

2.2. Storage issues

The resins and curatives must be heated to processing temperatures for several hours prior to mixing. In practice, however, these materials are kept at the processing temperatures indefinitely, raising the possibility of degradation with time. Of the 828, DEA, and Z reactants, we would expect Z to be most sensitive to aging since aromatic amines are known to oxidize. Indeed, Z does darken considerably with time at temperature, which has been suggested repeatedly over the years as a sign of potential degradation. The historical answer to this question states that aromatic amines are notorious for slight oxidation that causes inordinate color change; that is, a small amount of oxidation in aromatic amines produces a great color change. Given the previous discussion in this paper, measurement of the glass transition temperature of the Z-cured epoxy as a function of Z aging time would answer this question definitively.

A new lot of Z curative was aged in an oven for 14 days at 120^{o}C. Z is routinely stored at 54^{o}C, so 120^{o}C represents an accelerated aging condition. Assuming a standard activation energy for the aging chemistries, 14 days at 120^{o}C corresponds to approximately 10 months at 54^{o}C.

The glass transition temperature was measured with a TA differential scanning calorimeter (DSC) at a heating rate of 5^{o}C/min. While the signature of Tg is a step change in heat capacity, asymmetric cooling and heating rates also produce a "physical aging" peak at Tg resulting from the viscoelastic nature of the polymer. In Fig. 12, the physical aging peak temperatures are shown for both the unaged and aged 828/Z epoxies cured according to Table 5. Even with the severe aging history, no significant change in Tg is apparent.

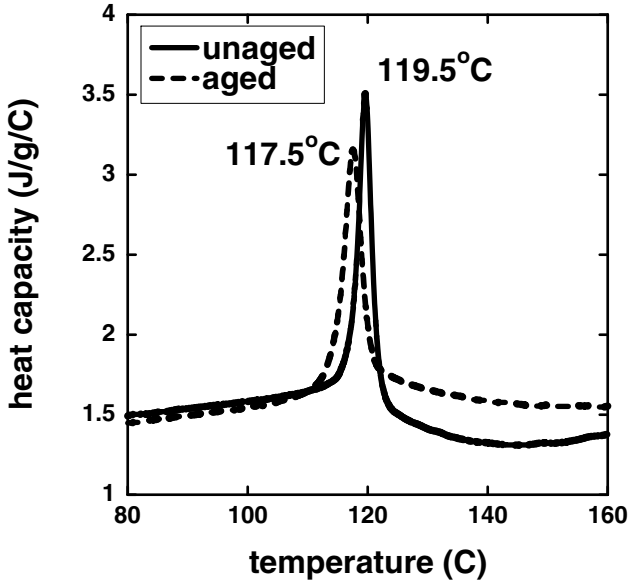

Fig. 12: Change in Tg in 828/Z after the Z curative was aged at 120ºC for 14 days.

3. Sensitivities of material properties to selected weighing/mixing/ degassing/pouring issues

3.1. Weighing of epoxy reactants

Reactant weights during processing are controlled to ±1%. These weight constraints coupled with the allowed bounds in incoming material functionalities could result in stoichiometric (moles curative/moles epoxy) variations of ±5% in the worst case. To test the effect of such variations, samples of 828/DEA and 828/Z were mixed at -5%, +5%, and +10% of the nominal stoichiometric ratios (12 pbw DEA or 20 pbw Z to 100 pbw 828). Since the samples were made with each reactant obtained from only one container, there will be no variations in stoichiometry from differences in incoming material within these families, so the variations examined represent modest over-tests. The weights were controlled in these batches to stringent requirements (±1mg for roughly 20g batch size using a calibrated analytical balance). The DEA samples were cured isothermally at 71ºC for 24 hrs, and the Z samples were cured for 1 hr at 25ºC, ramped to 93ºC in 10 hrs, and cured 10 additional hrs at 93ºC. Again, the glass transition temperature was examined since it is the most sensitive cured property, as described above.

The Tg's of the cured materials were measured by DSC at a heating rate of 5ºC/min, and Tg was again defined as the maximum in the physical aging peak. The DSC traces are shown in Figs. 13 and 14. There is no discernable difference between the Tg's of the Z-cured epoxy at ±5% ratios. Even at twice the maximum allowed variance, Tg decreases by a mere 1.5ºC.

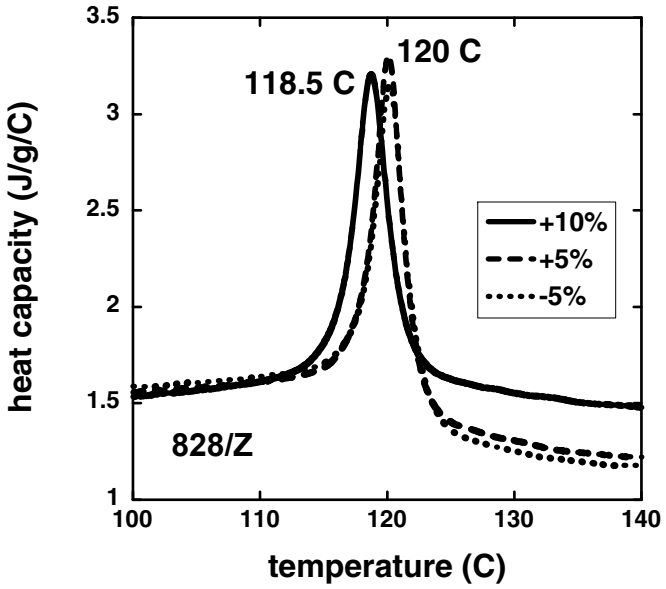

Fig. 13: DSC Tg's of 828/Z at off-stoichiometric ratios (gZ/g828).

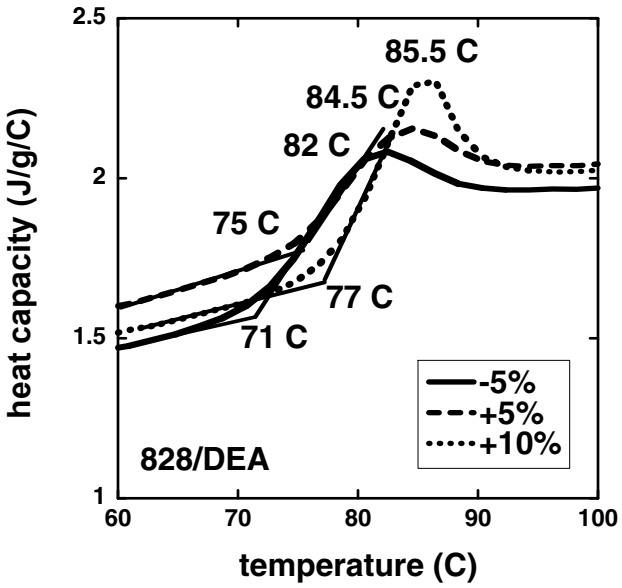

Fig. 14: DSC Tg's of 828/DEA at off-stoichiometric ratios (gDEA/g828).

Clear extraction of "Tg" for the DEA-cured epoxy is more difficult since the aging peak is less distinct. Tg is defined as the maximum in the aging peak or the onset of Tg are labeled in Fig. 14 and plotted in Fig. 15 as a function of stoichiometric ratio.

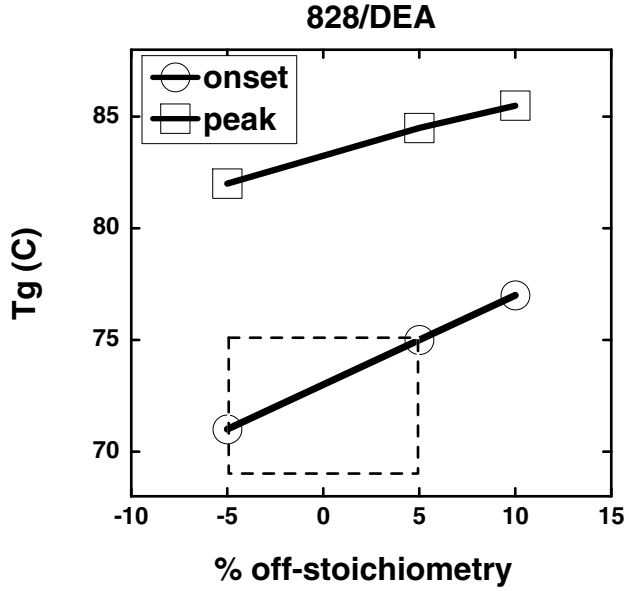

Fig. 15: Tg of 828/DEA as a function of stoichiometric ratio (gDEA/g828).

The dotted lines outline a region defined by the allowed stoichiometric ratios (±5%) and twice the standard deviation on Tg's measured from samples of 828/CTN/DEA/GMB taken from each generator poured on the production floor. The variations in Tg's from this study match those variations seen in actual units. The accuracy of the DSC test for measuring Tg's will be examined later in this report (see Section 4.3).

Of course, at some point, large variations in stoichiometric ratios will adversely affect Tg. Such large variations were investigated previously by Wischmann and Thomas.[5]

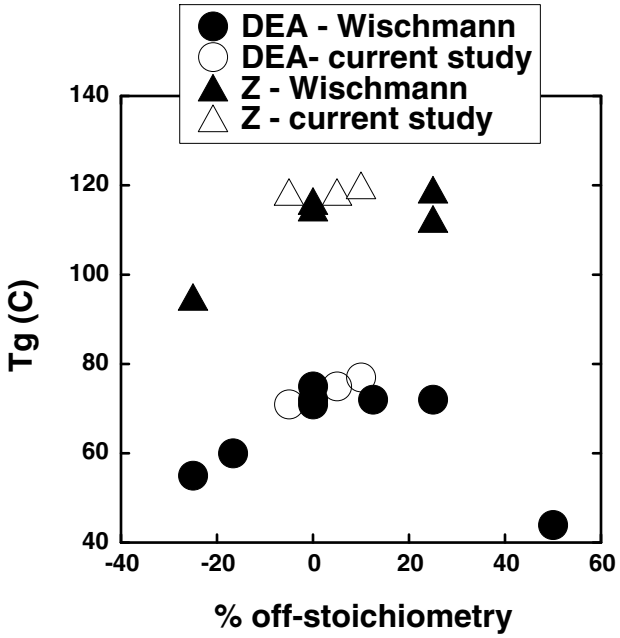

Fig. 16: Effect of large stoichiometric variations on DEA- and Z-cured epoxies.

It appears that larger variations in Tg occur when too little curing agent is added. That is, a 20% excess of curing agent has minimal effect on Tg, whereas 20% lack of curing agent can cause a 15C drop in Tg.

Stoichiometric variations cannot only affect Tg but can affect the reaction rate itself. DSC traces of the reaction rates are shown in Figs. 17 and 18.

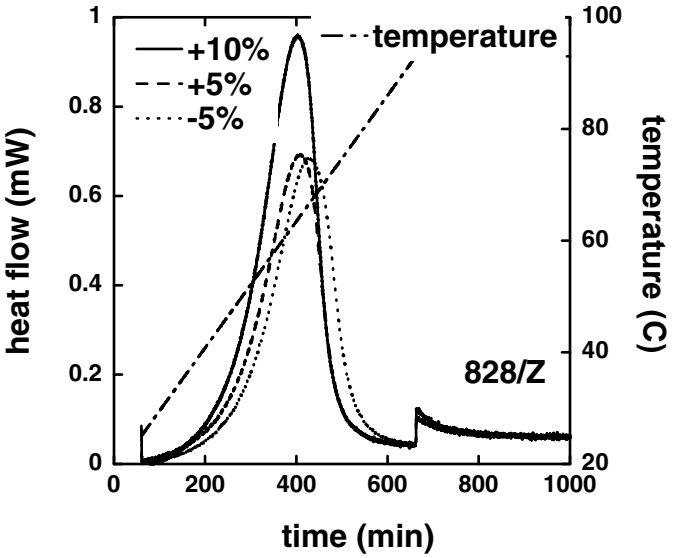

Fig. 17: DSC reaction rates for Z at off-stoichiometric ratios.

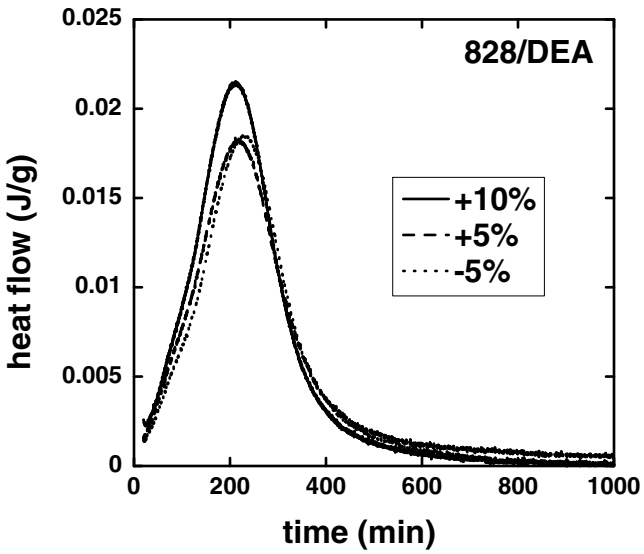

Fig. 18: DSC reaction rates for DEA at off-stoichiometric ratios.

The maximum of the autocatalytic reaction peak varies in time by only 5% for both systems even including the +10% variation. The reaction exotherms are affected only by the +10% variation and increase by approximately 30% in the Z system and 15% in the DEA system. However, this increase is not representative of our filled systems where the volume fraction of filler is almost 50%. Therefore,

the actual percent changes in exotherm for actual encapsulants should be reduced by a factor of two.

We have shown previously[6,7] that the viscosity of unfilled, curing epoxies is Newtonian and dependent on temperature and extent of reaction in the following fashion:

$$\eta = \eta_{ref}\left[10^{-\frac{C_1(T-T_{ref})}{C_2+T-T_{ref}}}\right]\left[\frac{p_c^2-p^2}{p_c^2}\right]^{-4/3} \qquad (1)$$

where C_1, C_2, and T_{ref} are the standard "WLF" parameters[8] for this system, η_{ref} is the viscosity of the unreacted system at the reference temperature, T_{ref}, and p_c is the extent of reaction at the gel point where the viscosity diverges. The temperature, T, and extent of reaction, p, dependencies are separable in this relationship. The reference temperature, T_{ref}, is usually defined as Tg, but Tg (or T_{ref}) increases with extent of reaction as well. A convenient fitting function for this increase prior to the gel point is given by[9]

$$T_g(p) = \frac{T_g^o}{(1-Ap)} \qquad (2)$$

where Tg^o is Tg of the unreacted system and A is a constant. Note that the increase in Tg with extent of reaction will not be affected by the small stoichiometric variations investigated in this study since the extent of reaction was unaffected.

Therefore, we would conclude from this subsection that the current bounds on reactant weights during processing are quite tight, and no variations in material properties arising from variations within these bounds would be significant. In fact, the data indicate that it would not be objectionable if these bounds were doubled.

3.2. Weighing of fillers

Weights of fillers are also controlled to within ±1%. While it is well established that large, inert, particulate fillers do not affect the Tg or cure kinetics

of the underlying epoxy,[10] they do obviously affect both the liquid and solid properties of the encapsulant.

The viscosities of our filled encapsulants are not always Newtonian. While GMB-filled viscosities are fairly Newtonian, the alumina-filled viscosities can be severely shear thinning.[7] Nevertheless, the scaling of all viscosities with volume fraction filler at constant test conditions (rate, temperature,…) is similar.[7]

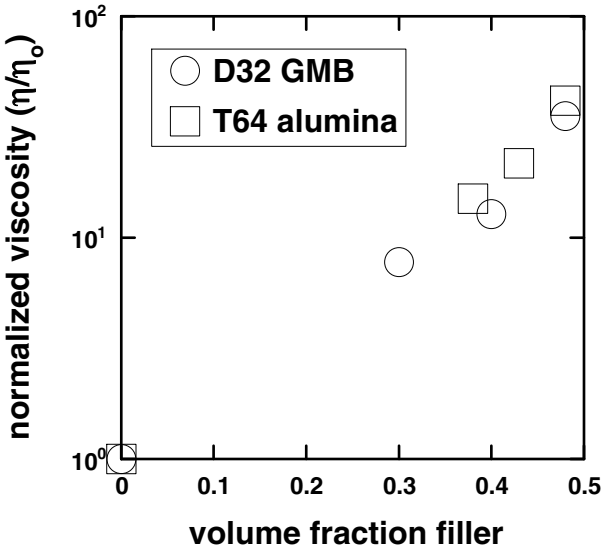

Fig. 19: Dependence of the viscosity of filled systems (GMB or alumina in 828 epoxy) normalized to the unfilled resin viscosity at the same test conditions.

Fig. 19 can be expanded around the region of interest to our encapsulants. For example, the volume fraction of alumina filler in the 828/Z/Alox encapsulant is nominally 43.3% (assuming densities of 3.92 g/cc and 1.2 g/cc for the filler and resin respectively).

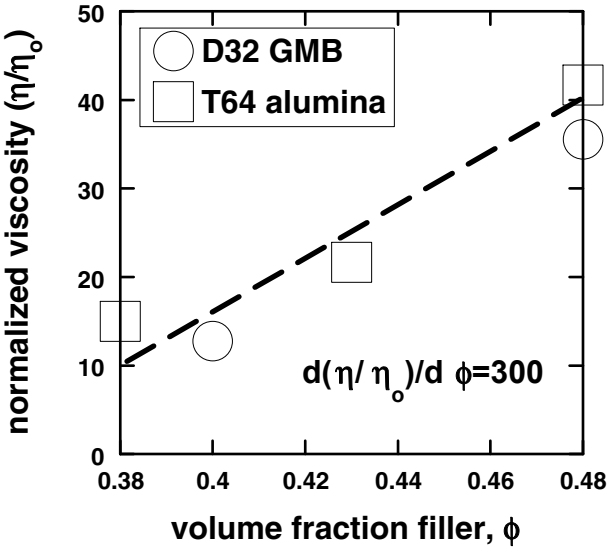

Fig. 20: Expanded view of Fig. 19.

Weighing errors of 1% in filler and resin would result in variations in volume fraction of at most 0.5%. From Fig. 20, these weighing errors translate in ±5% variations in the viscosity of the filled, liquid resin. Returning to Fig. 5, the viscosity of curing 828/Z/T64alox (43vol%) could vary by an order of magnitude due to lot-to-lot variations in the incoming alumina. Therefore, ±0.5% variations due to weighing errors appear small given the historical variations that must have been encountered over the years. Again, the data suggest that even doubling the bounds on weighing fillers would not be objectionable considering viscosity alone. Sensitivities to mechanical properties will be considered next.

Alumina-filled epoxies should show more significant changes in mechanical properties with volume fraction than the corresponding GMB-filled systems since the alumina particulates have much more disparate properties than the resin. In fact, the shear moduli for the unfilled 828/DEA and 828/DEA/GMB encapsulants are almost identical.[11] Therefore, the discussion of weighing sensitivities will be discussed from the perspective of the alumina-filled encapsulants.

The linear shear modulus and volumetric coefficient of thermal expansion are plotted against volume fraction of alumina filler in Fig. 21 for the 459, "Z-replacement" epoxy.

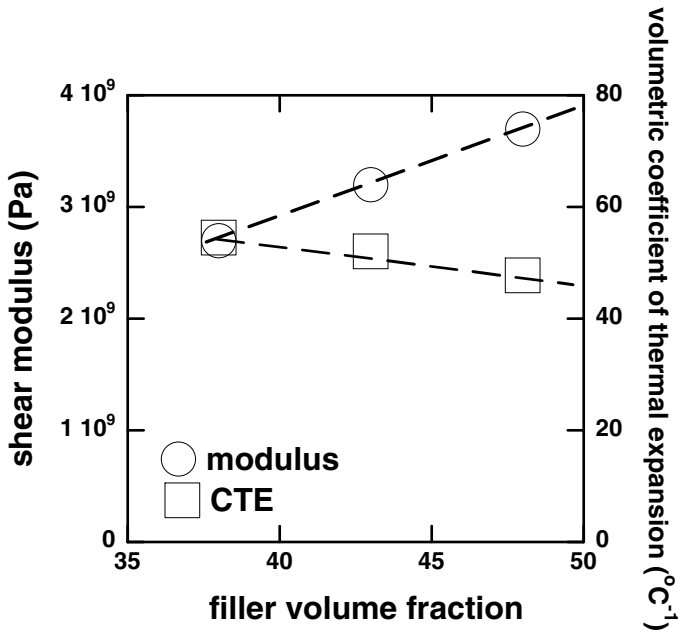

Fig. 21: Linear elastic properties for the 459/T64 alumina encapsulant as a function of volume fraction alumina.

The variations in properties from ±0.5vol% weighing errors are ±1% and ±2% for the CTE and modulus respectively. Typically, the product of these two properties indicates the propensity to generate stresses during thermal cycles. Since the CTE decreases with increasing filler fraction while the modulus increases leading to competing trends, the product itself varies insignificantly over the weighing bounds.

One measure of the sensitivity of nonlinear encapsulant response to filler loading levels is the room temperature compressive yield stress shown in Fig. 22 again for the 459/T64 alumina encapsulant.

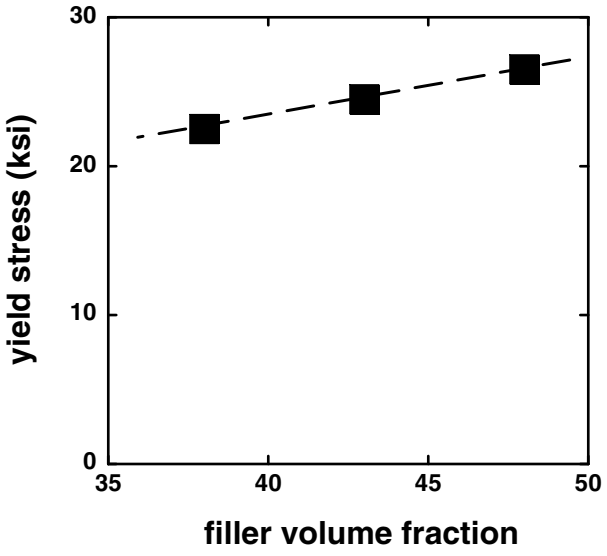

Fig. 22: Room temperature, compressive yield stress of the 459/T64 alumina encapsulant as a function of volume fraction alumina.

Even here, the nonlinear yield stress varies by less than 2% over the range in allowed filler loading.

The dependencies of the ultimate properties, both adhesive and cohesive, on filler fraction are plotted in Figs. 23 and 24. Critical adhesive shear tractions were measured by napkin ring tests at room temperature. The cohesive fracture toughnesses were measured at room temperature using pre-cracked, three-point bend samples.

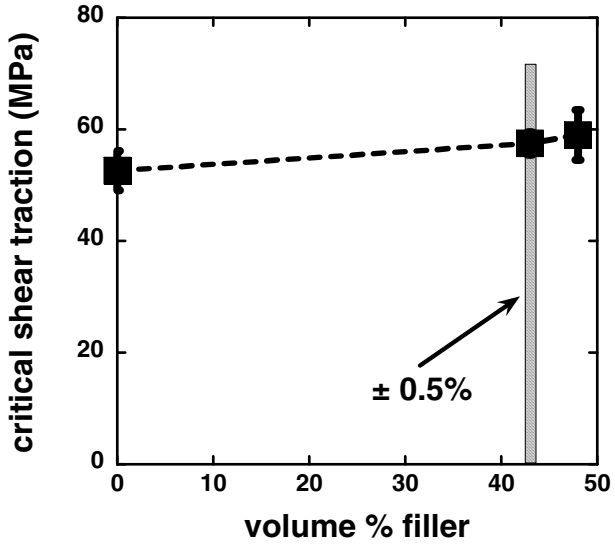

Fig. 23: Dependence of the adhesive strength in shear on volume fraction of alumina filler in 459 epoxy.

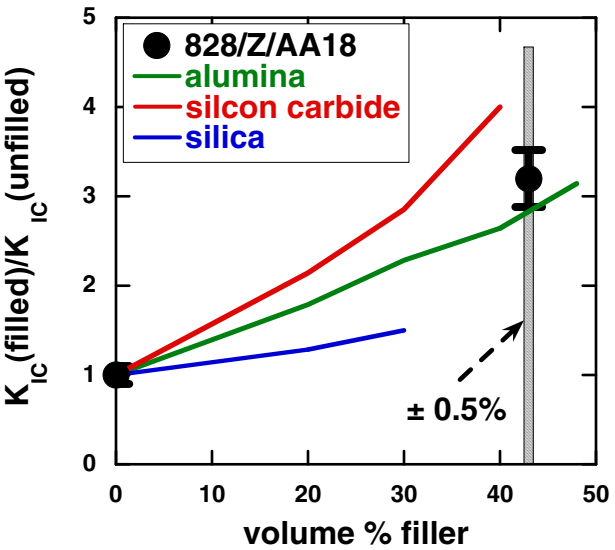

Fig. 24: Dependence of the normalized cohesive stress intensity factor on volume fraction of alumina filler in 459 epoxy (symbols) and literature values (lines).[12]

Adhesive strength is very insensitive to filler loading level, perhaps since the particles are excluded from the region very close to the interface. The cohesive strength does increase with increasing volume fraction of filler; however, variations of ±5% in filler volume fraction again result in very small changes in the fracture toughness.

The sensitivities of high rate and dielectric responses to alumina filler fraction and type are being gathered in a concurrent program[3]. Results indicate that the sensitivity of the high rate response of alumina-filled epoxies is similar to the quasi-static sensitivity. Novel high rate ramp tests have been performed using the Z-facility on the "459", Z-replacement encapsulant.[3] The raw data were reduced by Dennis Hayes to produce the pressure-volume relationships shown in Fig. 25.

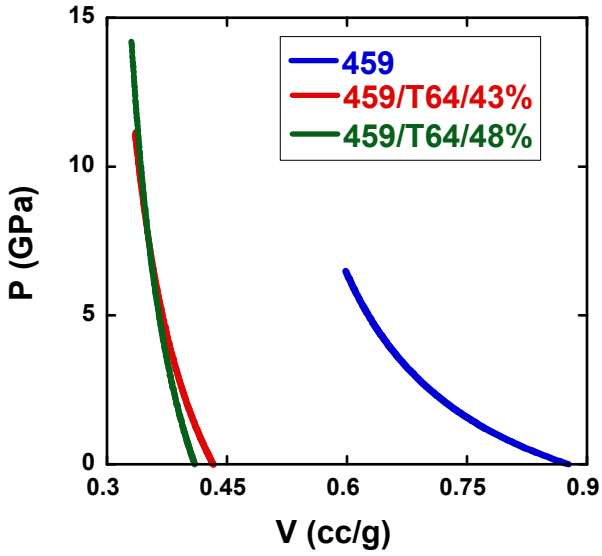

Fig. 25: Pressure-volume relationships for the alumina-filled, Z-replacement encapsulant at various filler volume fractions extracted from high rate ramp tests using the Z-facility.

Little sensitivity is observed for volume fraction variations of 5%, so the P-V responses for ±0.5% variations would be virtually identical plotted as in Fig. 25.

From the preceding discussion, it is clear that the tolerances on filler weights are quite tight. Again, it would seem that doubling the present bounds would be acceptable.

3.3. Temperature control during weighing/mixing/degassing/pouring

Bounds on oven and vacuum chamber temperatures are typically ±3ºC. This temperature range will affect both the viscosity of the liquid encapsulant and its reaction rate, which in turn will have an additional effect on the viscosity. The temperature dependence of the filled encapsulants follows that of the unfilled reactants. In Fig. 26, the temperature dependent viscosities of the epoxy resin (828), the rubber toughened epoxy resin (828/CTBN), and the unreacted but mixed 828/DEA mixture (i.e., short time so no reaction) are plotted.

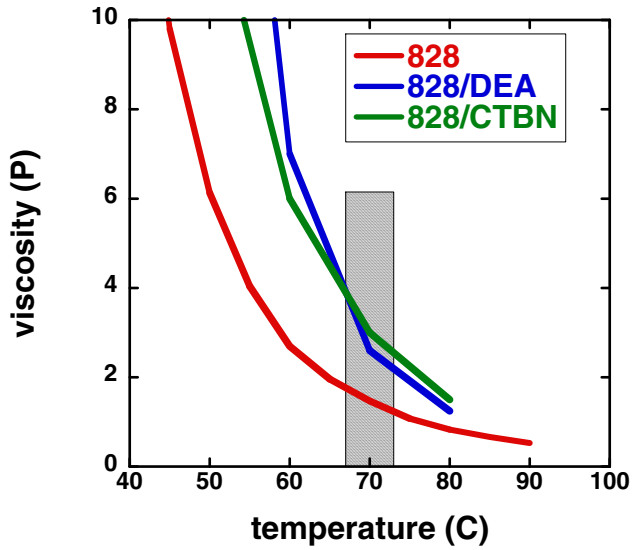

Fig. 26: Temperature dependent viscosities of several epoxy liquids.

The shaded region indicates the prescribed ±3ºC temperature bound about 70ºC. Surprisingly, the viscosities are quite temperature sensitive, resulting in variations in viscosity of 50% or greater.

While this variation may be concerning, the actual variations during mixing/degassing/pouring can be much larger. Since the mixing bowls are not insulated, temperature decreases of 10ºC or more have been recorded in the development lab. The process floor does not even monitor mixing bowl temperature so actual temperature variations are unknown. However, the data in Fig. 26 suggests that viscosities could vary by a factor of five during our mixing/degassing/pouring operations. This estimate does not account for more complex variations in viscosity arising from changes in extent of reaction accompanying temperature fluctuations, which will be discussed later.

What would be the consequences of relatively large variations in viscosity during this early stage of the encapsulation process? Since the largest temperature variations are due to the uncontrolled mixing bowl temperature, one might expect degassing characteristics to be affected. Improper degassing due to higher viscosities could result in voids and potential dielectric breakdown initiation sites. These large variations in viscosity from the uninsulated mixing bowls would probably not affect pouring, however. The thermal mass of the mold is so great and the thermal transport surfaces areas so large, that one anticipates the encapsulant would almost immediately equilibrate to the mold temperature set by the oven temperature. From the discussion above, the ±3°C bounds on the oven temperature could lead to 50% changes in the encapsulant viscosity, which are still fairly large.

Temperature variations directly affect the viscosity as detailed above, but they also produce a secondary effect on viscosity by changing the rate of reaction. Examine the DEA-cured epoxy as an example. The reaction rate equation, documented elsewhere,[13] can be integrated to assess the effect of ±3°C temperature measurement or control errors on the extent of reaction (Fig. 27).

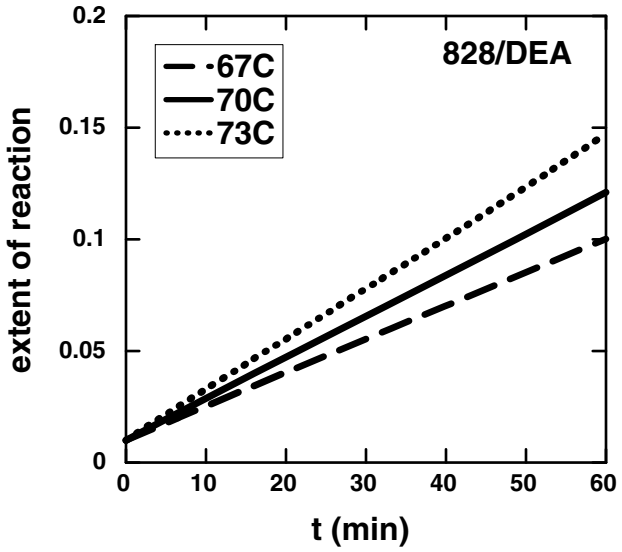

Fig. 27: Changes in the extent of reaction for the 828/DEA epoxy for variations of ±3°C in oven temperature.

Using Eqs. 1 and 2, the subsequent effects on the evolving glass transition temperature and viscosity through the first hour of cure can be predicted (Figs. 28 and 29 respectively).

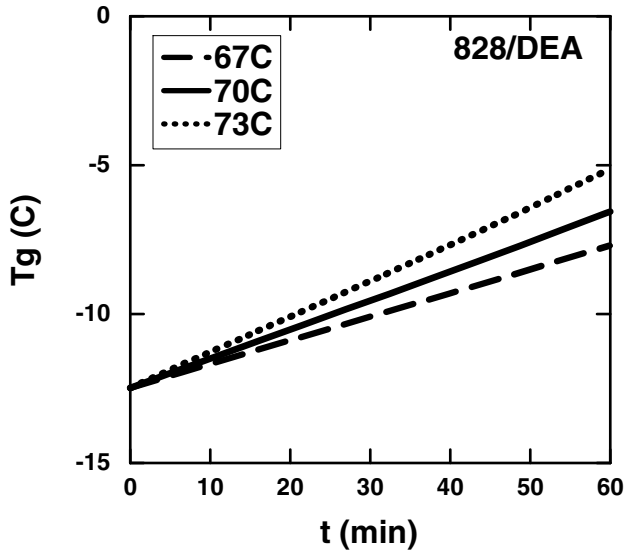

Fig. 28: Effect of variations of ±3°C in oven temperature on the evolving glass transition temperature.

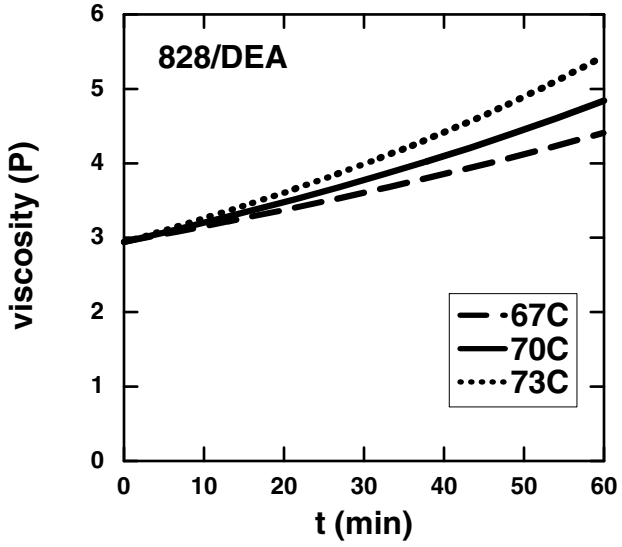

Fig. 29: Effect of variations of ±3°C in oven temperature on the evolving viscosity.

The viscosity changes by only ±10%. Therefore, the effect of changes in extent of reaction due to temperature variations on viscosity are not nearly as severe as the direct effect of temperature on viscosity shown in Fig. 26. However, this primary effect is so great that it would be prudent to investigate methods to monitor and minimize temperature variations during the mixing/degassing/pouring stages of processing.

4. Effect of selected curing issues on material properties

4.1. Temperature control during cure

Temperature variations during cure can affect generators in two ways. First, very poor temperature control could affect the final extent of reaction of the encapsulant and thereby possibly affect encapsulant properties. Second, stresses generated during cure depend on the entire temperature profile. Cure stresses are generated from two primary sources: volumetric shrinkage accompanying each chemical reaction and relative expansion of the polymer as temperature increases. The cure shrinkage has been shown to be proportional to the extent of reaction,[6] which itself will depend on the temperature profile. The thermal expansion of the polymer, due to its higher coefficient of thermal expansion relative to metals and ceramics, is operative only during ramps.

To estimate the sensitivity of these two effects to modest variations in the cure thermal history, we will calculate the extent of reaction for the DEA-cured, GMB-filled rubber toughened epoxy (828/CTBN/DEA/GMB) using the reaction rate equation previously determined[13] and examine cure strains for a stress-free volumetric deformation

$$\Delta_v = \alpha\left(T - T_{gel}\right) + \beta(p - p_c) \qquad (3)$$

where α = 330 ppm/C is the CTE,[14] β = - 0.06 is the total cure shrinkage,[13] p_c = 0.65 is the extent of reaction at the gel point,[13] and Tgel is the temperature at the gel point, which varies for the different cure schedules. The experimental set-up

shown in Fig. 8 used to compare mold release effectiveness can also be used to determine cure stresses. If the disk to which the strain gauges are attached were very thin and the sides of the tube were mold released, Eq. (3) would estimate the measured strains fairly well. In practice the disks are not infinitely thin and the epoxy does adhere to the steel walls so Eq. (3) will predict strains that are too high. Nevertheless, the predictions can be used to assess sensitivities to variations in thermal profiles during cure.

Fig. 30 shows the predicted extents of reaction and Tg's for two cures. The "cold" cure plunges to 25°C and ramps to 93°C while the "hot" cure plunges to 31°C and ramps to 99°C.

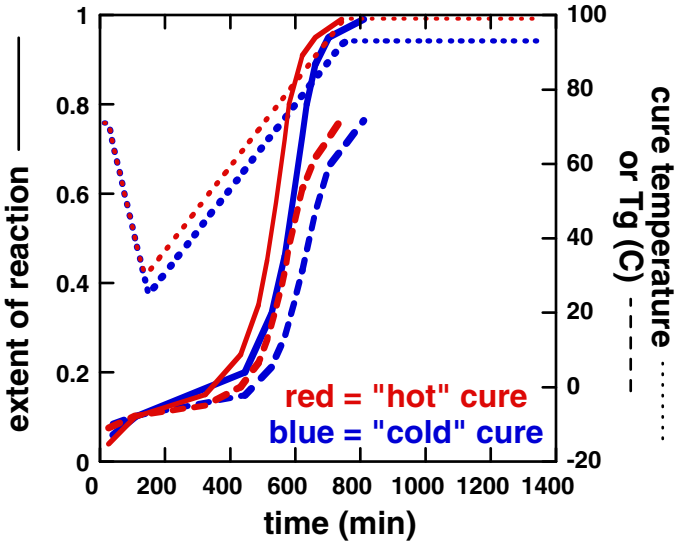

Fig. 30: Variation in the extent of reaction and Tg predicted for a DEA-cured epoxy under two different temperature curing profiles.

It is clear that both profiles cure the epoxy to the same final state. In fact, only very gross deviations from the prescribed cure profile would incompletely cure the epoxy. The predicted cure strains for the two profiles are plotted in Fig. 31.

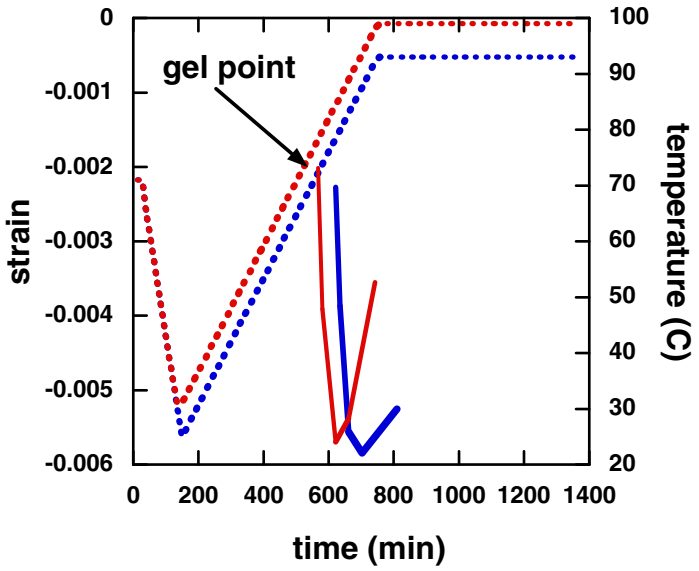

Fig. 31: Variation in the cure strains predicted for a DEA-cured epoxy under two different temperature curing profiles.

These small variations in temperature history have no profound effect on the predicted cure strains.

However, are these predictions accurate? Strains measured in the apparatus depicted in Fig. 8 are compared to the strains predicted by Eq. 3 in Fig. 32.

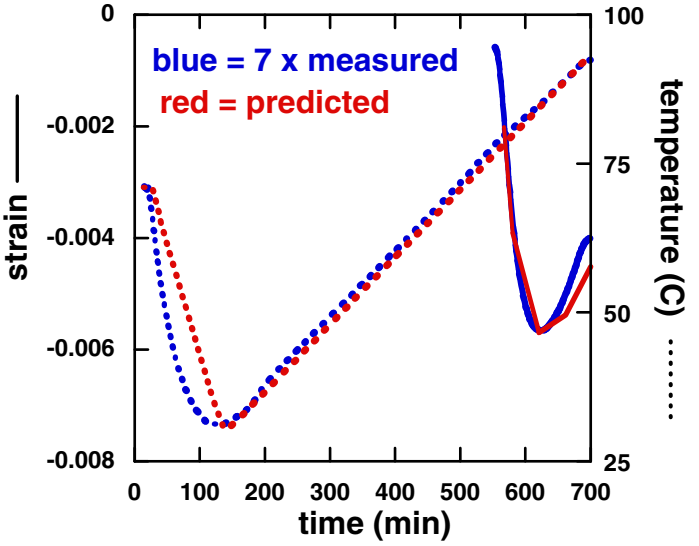

Fig. 32: Measured and predicted strains during cure.

The magnitude of the predicted strains are roughly seven times to high, which is not unexpected for such a simplistic calculation; however, the qualitative shape of strain evolution is quite similar.

While the data presented above implies that reasonable variations in the cure temperature profile do not significantly affect cure strains, very different profiles will generate completely different strains. Fig. 33 shows such dramatic differences for the 828/CTBN/DEA encapsulant cured by quite different profiles (red lines).

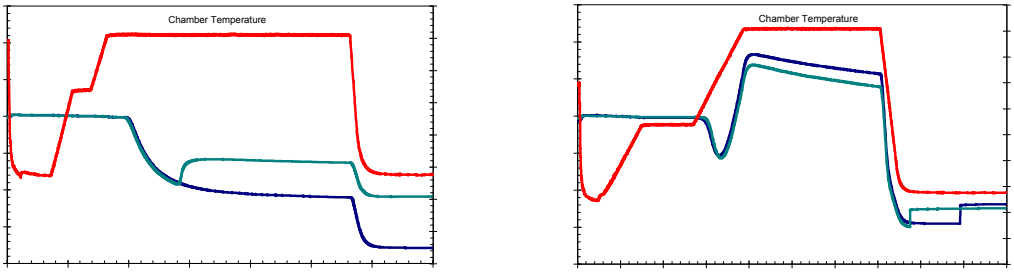

Fig. 33: Gross changes in the cure temperature history can generate significantly different cure stresses.

4.2. Effect of pressure during cure

Historically, generators have been cured under pressure to minimize the size of any trapped bubbles. The MC4368 generator is not pressure cured, however, for fears of tube deformation. Indeed, strain gauges have been attached to both the head and sides of MC4277 tubes (used in MC4368 generators) to measure deformations during pressurization. In Fig. 34, the strain gauge readings during a series of increasing pressure ramps are shown. While the tube withstood pressures three times greater than the historical value of 80 psig, irreversible yielding was observed, most noticeably on the top lid.

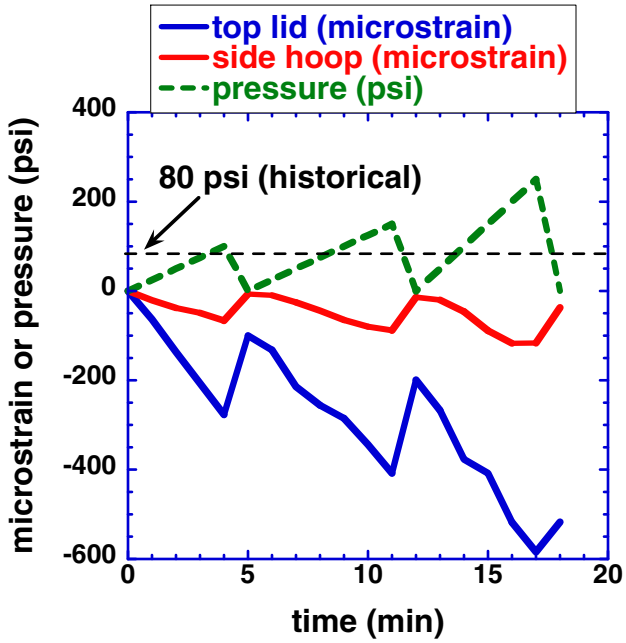

Fig. 34: Strain gauge readings on the MC4277 tube during pressurization.

The new MC4300 tube is scheduled to be pressure cured at 80 psig, and we can assess the sensitivity of bubble size to the applied pressure. In previous tests,[15] a bubble, trapped at atmospheric pressure within a curing epoxy, was periodically subjected to lower pressure in a vacuum tank. The change in the bubble size was monitored as the epoxy cured. This change in size followed the ideal gas law when the epoxy was liquid, but after the gel point, the change in size diminished until the epoxy modulus was so large that no change was measurable (Fig. 35).

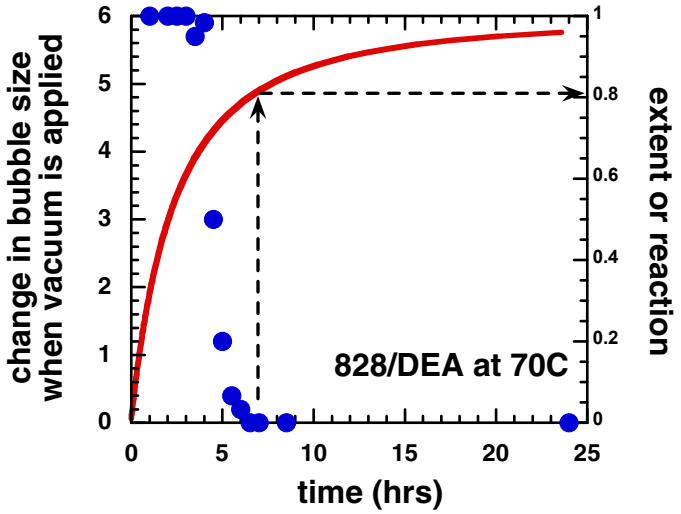

Fig. 35: Effect of epoxy cure on the change in bubble size when a vacuum is applied.

To assess sensitivities, it is useful to fit these results mathematically. Assume that the epoxy is elastic with modulus, E, that the gas in the bubble obeys the ideal gas law, and that the surface tension, γ, of the epoxy is independent of the extent of reaction (all reasonable assumptions). The pressure inside the bubble, P_{in}, determines the bubble radius, R.

$$P_{in} - P_{out} = \frac{4E}{3}\frac{R - R_o}{R_o} + \frac{2\gamma}{R} \tag{4}$$

where P_{out} is the pressure outside the bubble in the epoxy, and R_o is the initial radius of the bubble defined by the ideal gas law during processing under a vacuum of P_{vac}.

$$P_{in} = \left(P_{vac} + \frac{2\gamma}{R_o}\right)\left(\frac{R_o}{R}\right)^3 \tag{5}$$

Combining Eqs. 4 and 5 results in

$$\left(P_{vac} + \frac{2\gamma}{R_o}\right)\left(\frac{R_o}{R}\right)^3 = \frac{4E}{3}\left(\frac{R - R_o}{R_o}\right) + P_{out} + \frac{2\gamma}{R} \tag{6}$$

Let us first assess the significance of surface tension (at most 40mJ/m^2 for epoxies). Since surface effects will be more important as the bubble radius decreases, assume the pressurized bubble radius is 10 mils, a bit smaller than theresolution of current X-ray analyses. The size of a void, trapped at the processing vacuum of 1 Torr, which would result in a R=10 mil bubble in the pre-gel epoxy pressurized to 80 psig, can be calculated from Eq. (6)

$$\frac{R_o}{R} = \left[\frac{P_{out} + \frac{2\gamma}{R}}{P_{vac} + \frac{2\gamma}{R_o}} \right]^{1/3} \tag{7}$$

and results in a value of R_O=4.1 mm. The solution neglecting surface tension is 4.2 mm, a negligible effect even for this smallest of observable bubbles.

Neglecting surface tension, then, Eq. 6 can be used to predict the experimental results shown in Fig. 35.

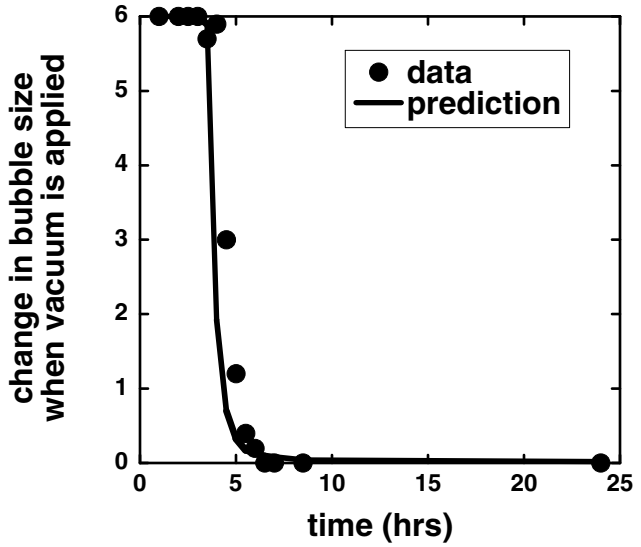

Fig. 36: Predictions of the data in Fig. 33 using Eq. 6.

The fit is quite good.

Summarizing, then, the gas inside voids greater than R=10 mils can be modeled with the ideal gas law. Surface tension effects are negligible. Also, variations in the curing pressure will only be important for a few hours after the gel point, roughly 4 to 7 hrs for the DEA-cured epoxies as shown in Fig. 36. At times less than 4 hours, the epoxy is liquid and effects of pressure fluctuations are recoverable. After 7 hours, the epoxy modulus is large enough that pressure fluctuations would not be large enough to change the bubble size. Even in the critical range of 4 to 7 hours, an overestimate of the sensitivity of bubble size to pressure is given by the ideal gas law.

$$\frac{R}{R_o} = \left(\frac{P_{vac}}{P_{pressure}} \right)^{1/3}$$

Changes of ±10 psig in pressure about the nominal value of 80 psig result in less than 5% change in bubble size. In fact, pressure cure itself reduces bubble size by less than a factor of 2. Therefore, it should be regarded as reducing voids trapped during processing that are near the limit of detection to sizes that can no longer be detected. As a final point, a bubble in a fully cured epoxy using no pressure cure that is at the limit of detection (R=10 mils) would have had a radius of 1.6 mm at 3 Torr. These are enormous trapped voids.

4.3. Post-cure tests

A series of analytical tests are performed on every generator poured and cured. The glass transition temperature, percent nitrogen, and residual ash are measured, in theory, to assess the curing, stoichiometry, and filler content respectively. As seen in Fig. 16, the glass transition temperature can also be affected by stoichiometry, so the Tg and %N2 tests are somewhat redundant. Historically, very few anomalies have been recorded; however, "drifts" in the mean occur, which have led to speculations that "process controls are lax". To understand the significance of such drifts and anomalies, it is necessary to first define the sensitivities of these tests.

A series of DEA-cured, GMB-filled epoxies were prepared by Manny Trujillo of the Organic Materials laboratory with purposeful variations in the curative and filler weight fractions. Samples were made in roughly 1000g batches and component weights were carefully weighed to balance accuracy (0.1g) and

recorded. All samples were cured with the oven profile given in Table 5 using one lot of each component; therefore, no stoichiometric variations were introduced through incoming material variations. The samples were given to Mike Courtney and Janice Jacksits in the analytical department, for standard analyses[16] in three lots separated in time by a month each.

The results from the Tg tests are shown in Fig. 37.

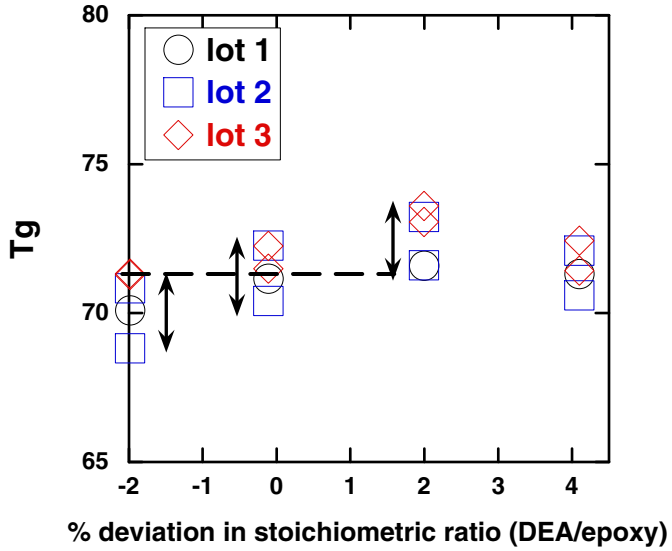

Fig. 37: Changes in Tg due to purposeful variations in DEA weight fractions.

Note that a ±1% weighing errors in both epoxy and curative lead to possible ±2% deviations in stoichiometric ratios. In this range, however, scatter in just these few measured values at each ratio is equivalent to the variation in average Tg at different ratios. That is, this test does not have the accuracy to assess if the encapsulant met the process weight requirements. However, it is useful for screening purposes to assess if a particular pour was severely out of specifications.

The results from the N2 tests are shown in Fig. 38.

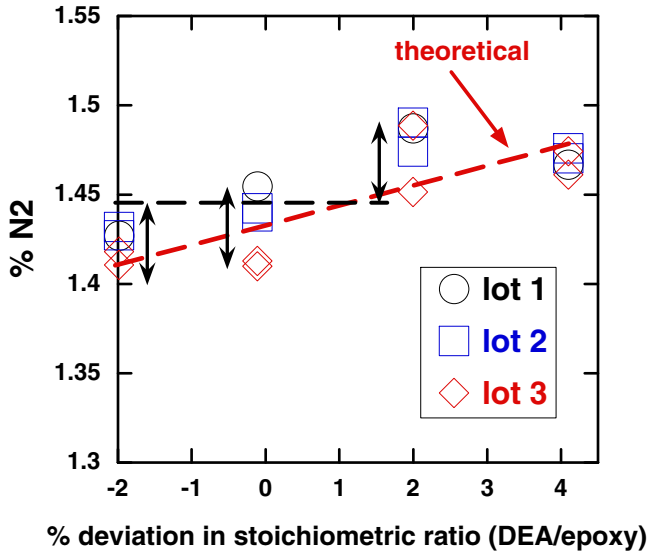

Fig. 38: Changes in % nitrogen due to purposeful variations in DEA weight fractions.

The theoretical %N2 is readily determined and plotted in Fig. 38 as well. As with the Tg measurements, scatter in the measured values at each ratio is equivalent to the variation in average %N2 at different ratios. Again this test cannot ensure proper process weight requirements but is useful for screening.

The results from the %ash tests are shown in Fig. 39.

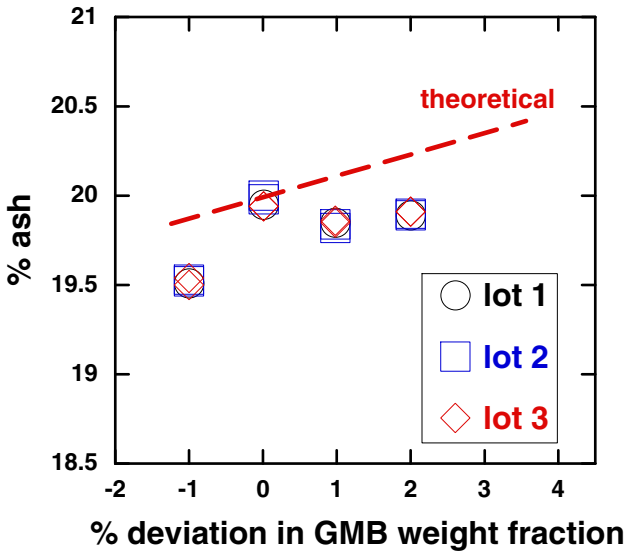

Fig. 39: Changes in % ash due to purposeful variations in GMB filler weight fractions

While little scatter is observed at each GMB weight fraction, the average values do not agree with the theoretical predictions (based on complete loss of organic mass and no loss of inorganic mass) leading one to wonder about the intrinsic accuracy of the test.

Historically, these tests have been performed on each encapsulation pour, but no limits were placed on the results. That is, test results are not used to accept or reject units, which appears reasonable in the light of Figs. 37-39. While these tests cannot ensure adherence to current process tolerances, they are the only encapsulation tests performed on the cured generator and might be considered useful as final screening tests. However, it is possible to consider elimination of the %N2 test for two reasons. First, as stated previously, it is somewhat redundant; Tg tests stoichioimetry as well. Second, while the Tg and %ash tests are quite simple to perform, %N2 is more laborious so its elimination would represent the greatest cost savings. Retaining Tg and %ash tests would still provide a final screening of the cured units with minimal cost.

5. Conclusions

An attempt was made to understand processing tolerances from a materials perspective by examining the dependence of properties key to generator functional on processing variables. Many processing parameters (e.g., reactant and filler weights) that are controlled extremely tightly were ineffective in generating changes in materials properties. However, some surprising sensitivities were discovered, such as the type of mold release solvent and transformer fabric, and the mixing/degassing temperature. Our investigations themselves do not constitute a complete coverage of all process sensitivities, but already, they seem to paint a different picture of our process than we may have had historically. Even though such studies should be continued, they are, by themselves, of little use if the conclusions drawn from them are not implemented. So, concurrent to these studies, discussions should begin to

understand how changes in process tolerances might be implemented along with changes in the process itself that may accompany the new tolerances.

Appendix

Compositions of the Epoxies Listed in Table 1

system	epoxy	curative
828/Z	diglycidyl ether of bisphenol A (DGEBA)	a mixture of aromatic amines
828/DEA	DGEBA	diethanolamine
SNL 459	DGEBA	a mixture of linear, multi-functional aliphatic amines
815/3300	DGEBA with monofunctional phenyl glycidyl ether diluent	a cycloaliphatic amine
862/T403	diglycidyl ether of bisphenol F (DGEBA)	a branched, multifunctional amine
826/3300	DGEBA	a cycloaliphatic amine
828/aniline	DGEBA	aniline
828/MEK	DGEBA	a peroxide catalyst for epoxy homopolymerization

References

(1) Weeks, T. S. Adolf, D. B., and McCoy, J. D. "Cohesive Failure in Partially Cured Epoxies", *Macromolecules*, **32**, p.1918-1922 (1999).

(2) J. P. Hickerson, Jr. and D. A. Paschal, Sandia Memo SC-RR-720766, October, 1972.

(3) Sandia Report SAND2005-6348, "Sensitivities of Alumina-Filled Encapsulant Properties to Filler and Resin Composition", Edited by Barb Wells and Doug Adolf, March, 2005.

(4) Sandia Report SAND2000-2185, "Compilation of Experimental Data Comparing the Effectiveness of Mold Release Coatings for Epoxy Encapsulants", T. R. Guess and M. E. Stavig, September, 2000.

(5) Sandia Report SAND89-1023, "An Evaluation of the Effects of Varying Composition and Processing on Several Encapsulating Resins", K. B. Wischmann and E. V. Thomas, January, 1991.

(6) Adolf, D. B., Martin, Chambers, R. S., Burchett, S. N., and Guess, T. R. "Stresses during thermoset cure", *J. Mat. Research*, **13**, p. 530-550 (1998).

(7) Sandia Report SAND97-2631, "Viscosities of Epoxy Encapsulants", D. B. Adolf, R. Strommen, and H. Johnson, November, 1997.

(8) *Viscoelastic Properties of Polymers*, J.D. Ferry, Wiley, 1980.

(9) Hale, A, Macosko, C. W., and Bair, H. E. *Macromolecules*, **24**, 2610 (1991).

(10) *Thermal Analysis*, B. Wunderlich, Academic, 1990.

(11) Sandia Report SAND89-0748, "Bulk and Shear Moduli of Epoxy Encapsulants", D. B. Adolf, C. K. Childress, and D. Hannum, August, 1989.

(12) Roulin-Moloney, Cantwell, W. J., and Kausch, H. H. Polymer Composites, 8, 314 (1987).

(13) Sandia Report SAND96-1458, "Measurement Techniques for Evaluating Encapsulant Thermophysical Properties During Cure", D. B. Adolf, June, 1996.

(14) Sandia Report SAND88-0777, "Coefficients of Thermal Expansion of Common Encapsulants", D. B. Adolf and C. K. Childress, July, 1988.

(15) Sandia Report SAND2003-4071, "Systematic Studies of the Neutron Generator Encapsulation Process", D. B. Adolf, S. T. Kawaguchi, M. E. Stavig, H. Arris, M. Trujillo, and D. Sanchez , November, 2003.

(16) The standard analyses measure the glass transition temperature (verification of oven cure), % nitrogen (verification of amine curative ratio), and % ash (verification of filler weight fraction).

Distribution:

NAME	MS	ORG
Duane Dimos	0887	01800
Dick Salzbrenner	0885	01820
Jim Aubert	0888	01821
Doug Adolf	0888	01821
Joe Lenhart	0888	01821
Mark Stavig	0888	01821
Brad Hance	0888	01821
Jill Glass	0889	01825
Mike Kelly	0958	02453
Howard Arris	0958	02453
Manny Trujillo	0958	02453-1
Carla Busick	0862	02701
Saskia King	0855	02701
Luis Paz	0515	02723
Todd Haverlock	0515	02723
Greg Neugebauer	0869	02723
Bob Stiers	0515	02723
Barb Wells	0862	02723
Tim Scofield	0335	02725
Steve Montgomery	0335	02725
Bob Welberry	0856	02710
Ruth Bargman-Romero	0856	02710
Cliff Renschler	0871	02720
John Sayre	0856	02730
Alan Parker	0876	02712
Bobby Baca	0862	02712
Lorraine Sena-Rondeau	0855	02719
Anne Lacy	0855	02719
Dolores Sanchez	0855	02719
Muhammad El	0869	02722
Bruce Bowles	0869	02722
Therese Ordonez	0869	02722
Michael Eatough	0867	02725

Neil Lapetina	0855	02732
Rich Antepenko	0871	02736
Michael Courtney	0871	02736
Central Technical Files	9018	8944
Technical Library (2 copies)	0899	4536